Numerical computations of a melting glass convection in the furnace

Tagami, Daisuke
Faculty of Engineering, Kyushu University

Tabata, Masahisa
Faculty of Engineering, Kyushu University

出版情報：Proceedings of the Seventh China-Japan Seminar on Numerical Mathematics, pp.149-160, 2006
バージョン：
権利関係：

MHF Preprint Series

Kyushu University
21st Century COE Program
Development of Dynamic Mathematics with High Functionality

Numerical computations of a melting glass convection in the furnace

D. Tagami & M. Tabata

MHF 2005-15

(Received April 8, 2005)

Faculty of Mathematics
Kyushu University
Fukuoka, JAPAN

Numerical computations of a melting glass convection in the furnace

Daisuke TAGAMI [a] and Masahisa TABATA [b]

[a] *Faculty of Engineering, Kyushu University*
Hakozaki, Higashi-ku, Fukuoka 812-8581, JAPAN
E-mail: tagami@mech.kyushu-u.ac.jp
[b] *Faculty of Mathematics, Kyushu University*
Hakozaki, Higashi-ku, Fukuoka 812-8581, JAPAN
E-mail: tabata@math.kyushu-u.ac.jp

A model of the melting glass convection in a furnace is computed by a finite element method based on the scheme mathematically justified. Some numerical results are demonstrated to investigate differences of the energy efficiency among some electrode configurations.

Keywords: melting glass, thermal convection, temperature-dependent coefficient, finite element method

AMS Subject classification: 76M10, 76R10, 65M60

1. Introduction

The design for glass furnaces with lower fuel consumption and with less CO_2 emission requires us to analyze precisely convection phenomena in the melting process. For a grasp of phenomena, the use of numerical computations is growing in acceptance, and there are many researches on the computations; see, for example, Choudhary [1], Curran [2], and Ungan and Viskanta [7]. Because the physical properties of raw glass materials depend on the temperature, physical coefficients should be treated with care in devising numerical schemes. Recently, we have mathematically justified a class of finite element methods for thermal convection problems with constant coefficients (see Tagami [5] and Tagami and Itoh [6]) or with temperature-dependent coefficients (see Tabata [3] and Tabata and Tagami [4]). In this paper we apply the scheme to numerical computations of the melting glass convection in the furnace.

Owing to the Boussinesq, the Rosseland (see Viskanta and Anderson [8]), and the infinite Prandtl number approximations, the raw material in the furnace is governed by thermal convection problems with the Joule heat. The equations are discretized by the backward Euler method in time and by the conforming finite elements in space. Temperature-dependent coefficients are treated by an approximation developed in [3] and [4]. Using the numerical scheme, we compute thermal convection phenomena in a model furnace with the Joule heat. We investigate differences among some electrode configurations on the temperature distribution, the convection patterns, and the energies given to the raw materials and passing through the throat.

2. A model problem

Figure 1 shows a model furnace to be considered, and its dimensions are listed in Table 1. This model is obtained by normalizing with its depth and rounding one given in [7]. Figure 1(a) shows

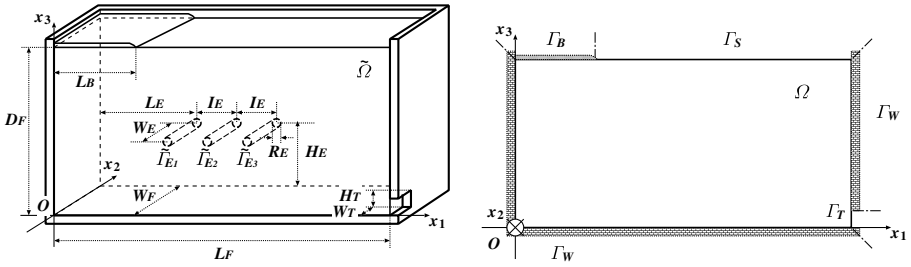

(a) A domain $\widetilde{\Omega}$: a half of the furnace.

(b) A domain Ω: the cross section on $x_2 = 0$ of the furnace.

Figure 1. A model furnace.

Table 1
The dimensions of the model furnace.

Physical quantity	Symbol	Dimension
Depth of Furnace	D_F	1
Length of Furnace	L_F	8
Width of Furnace	W_F	1
Height of Throat	H_T	0.3
Width of Throat	W_T	0.4
Radius of Electrodes	R_E	0.1
Width of Electrodes	W_E	0.5
Height of Electrodes	H_E	0.4
Interval between Electrodes	I_E	0.8
Length between Back Wall and Electrodes	L_E	3
Length of Batch	L_B	1

$\widetilde{\Omega}$, a half of the furnace, and Figure 1(b) shows Ω, the cross section on $x_2 = 0$ of the furnace. A raw material is fed into the furnace from the batch Γ_B, and flows out from the throat Γ_T. There is an air-fuel fired boundary Γ_S on the top of the furnace, and when an electric current flows between the electrode $\widetilde{\Gamma}_{E_1}$, $\widetilde{\Gamma}_{E_2}$, and $\widetilde{\Gamma}_{E_3}$, the Joule heat is generated in the furnace; for the simplicity, the electric current is assumed to be a direct current. The wall Γ_W is insulated.

The electric field is considered in the three-dimensional domain $\widetilde{\Omega}$. On the other hand, for the simplicity, the flow and the energy fields are considered only in the two-dimensional domain Ω. Thus the motion of raw materials can be written as follows: find the velocity u, the pressure p, the temperature

θ, and the electric potential ϕ,

$$(u, p, \theta) : \ \Omega \times (0, T) \to \mathbb{R}^2 \times \mathbb{R} \times \mathbb{R},$$
$$\phi : \ \widetilde{\Omega} \times (0, T) \to \mathbb{R},$$

such that

$$\begin{cases} -\nabla \cdot \big[\nu(\theta) D(u)\big] + \nabla p - \beta(\theta)\, \theta = 0 & \text{in } \ \Omega \times (0, T), \quad (2.1a) \\ \nabla \cdot u = 0 & \text{in } \ \Omega \times (0, T), \quad (2.1b) \\ \partial_t \theta + (u \cdot \nabla)\, \theta - \nabla \cdot (\kappa(\theta) \nabla \theta) = \dfrac{1}{2} \sigma(\theta) |\overline{\nabla \phi}|^2 & \text{in } \ \Omega \times (0, T), \quad (2.1c) \\ -\nabla \cdot (\widetilde{\sigma}(\theta) \nabla \phi) = 0 & \text{in } \ \widetilde{\Omega} \times (0, T) \quad (2.1d) \end{cases}$$

with the boundary conditions for the flow field

$$\begin{cases} u = u_D & \text{on } \ \Gamma_W \cup \Gamma_B \times (0, T), \quad (2.2a) \\ \tau(u, p, \theta) = 0 & \text{on } \ \Gamma_T \times (0, T), \quad (2.2b) \\ u \cdot n = 0, \quad \tau(u, p, \theta) \cdot t^{(1)} = 0 & \text{on } \ \Gamma_S \times (0, T), \quad (2.2c) \end{cases}$$

for the energy field

$$\begin{cases} \theta = \theta_D & \text{on } \ \Gamma_B \cup \Gamma_S \times (0, T), \quad (2.3a) \\ \dfrac{\partial \theta}{\partial n} = 0 & \text{on } \ \Gamma_T \cup \Gamma_W \times (0, T), \quad (2.3b) \end{cases}$$

and for the electric field

$$\begin{cases} \phi = \phi_D & \text{on } \ \widetilde{\Gamma}_E \times (0, T), \quad (2.4a) \\ \dfrac{\partial \phi}{\partial n} = 0 & \text{otherwise}, \quad (2.4b) \end{cases}$$

and with the initial condition

$$\theta = \theta^0 \quad \text{in } \ \Omega \ \text{ at } \ t = 0, \tag{2.5}$$

where $\widetilde{\Gamma}_E$ denotes a union of the electrode boundaries, $\widetilde{\Gamma}_{E_1} \cup \widetilde{\Gamma}_{E_2} \cup \widetilde{\Gamma}_{E_3}$; n an outward unit normal, and $t^{(1)}$ a unit tangent;

$$u_D : \ \Gamma_W \cup \Gamma_B \times (0, T) \to \mathbb{R}^2,$$
$$\theta_D : \ \Gamma_B \cup \Gamma_S \times (0, T) \to \mathbb{R}, \quad \phi_D : \ \widetilde{\Gamma}_E \times (0, T) \to \mathbb{R}$$

a set of boundary velocity, temperature, and electric potential;

$$\theta^0 : \ \Omega \to \mathbb{R}$$

an initial temperature;

$$(\nu,\, \kappa,\, \sigma,\, \beta) : \ \Omega \times (0, T) \times \mathbb{R} \to \mathbb{R}^+ \times \mathbb{R}^+ \times \mathbb{R}^+ \times \mathbb{R}^2$$

a set of viscosity, thermal conductivity, electrical conductivity, and thermal expansion coefficient depending on x, t, and θ; $\tau(u, p,\, \theta)$ the surface stress defined by

$$\tau(u, p,\, \theta) \equiv \{-p\, I + 2\, \nu(\theta)\, D(u)\} \cdot n$$

with the identity tensor I; the value of $\overline{\nabla\phi}$ in (2.1c) is defined by

$$\overline{\nabla\phi}(x_1,x_3,t) \equiv \left(\frac{\partial\phi}{\partial x_1}(x_1,0,x_3,t), \quad 0, \quad \frac{\partial\phi}{\partial x_3}(x_1,0,x_3,t)\right)^T;$$

moreover, $\widetilde{\sigma}$ is defined by $\widetilde{\sigma}(x_1,x_2,x_3,t) \equiv \sigma(x_1,x_3,t)$.

3. Finite element approximation

Let X, Y, Q, and $\widetilde{X}$ be function spaces defined by $X \equiv H^1(\Omega)$, $Y \equiv X^2$, $Q \equiv L^2(\Omega)$, and $\widetilde{X} \equiv H^1(\widetilde{\Omega})$, respectively; let $(\,.\,,\,.\,)$ denote the inner product of $L^2(\Omega)$; let $\Psi(\theta)$, $V(u)$, and $\Xi(\phi)$ be function spaces defined by

$$\begin{aligned}
&\Psi(\theta) \equiv \{\psi \in X;\ \psi = \theta \ \text{ on } \ \Gamma_B \cup \Gamma_S\},\\
&V(u) \equiv \{v \in Y;\ v = u \ \text{ on } \ \Gamma_W \cup \Gamma_B,\ v\cdot n = 0 \ \text{ on } \ \Gamma_S\},\\
&\Xi(\phi) \equiv \{\xi \in \widetilde{X};\ \xi = \phi \ \text{ on } \ \widetilde{\Gamma}_E\},
\end{aligned}$$

respectively; and let Ψ, V, and Ξ be function spaces defined by $\Psi \equiv \Psi(0)$, $V \equiv V(0)$, and $\Xi \equiv \Xi(0)$, respectively. We prepare bi- and tri-linear forms a_0, b, c_0, and c_1 defined by

$$\begin{aligned}
a_0(\nu;u,v) &\equiv 2\int_\Omega \nu\, D(u){:}D(v)\, dx \qquad \text{for } (\nu,u,v) \in L^\infty(\Omega)\times Y\times Y,\\
b(v,q) &\equiv -\int_\Omega q\,\nabla\cdot v\, dx \qquad \text{for } (v,q) \in Y\times Q,\\
c_0(\kappa;\theta,\psi) &\equiv \int_\Omega \kappa\,\nabla\theta\cdot\nabla\psi\, dx \qquad \text{for } (\kappa,\theta,\psi) \in L^\infty(\Omega)\times X\times X,\\
c_1(w,\theta,\psi) &\equiv \int_\Omega (w\cdot\nabla\theta)\,\psi\, dx \qquad \text{for } (w,\theta,\psi) \in Y\times X\times X.
\end{aligned}$$

We also prepare a bilinear form $\widetilde{c}_0$ by replacing the integral region Ω of c_0 by $\widetilde{\Omega}$.

We decompose the half furnace $\widetilde{\Omega}$ into a union of tetrahedra, and consider its cross section on $x_2 = 0$ as the triangulation of Ω. We introduce finite dimensional spaces X_h, Q_h, and $\widetilde{X}_h$ approximating X, Q, and $\widetilde{X}$, respectively. Let $\Psi_h(\theta)$ be a subspace of X_h approximating $\Psi(\theta)$; let $V_h(u)$ be a subspace of $Y_h \equiv X_h^2$ approximating $V(u)$; and let $\Xi_h(\phi)$ be a subspace of $\widetilde{X}_h$ approximating $\Xi(\phi)$.

Let τ be a time increment and $N_T \equiv [T/\tau]$ a total step number. The time $n\tau$ is denoted by t_n. We denote by θ^n the value $\theta(n\tau)$ at time step n and by $\overline{D}_\tau\theta^n$ the backward difference quotient $(\theta^n-\theta^{n-1})/\tau$.

Let us denote by $\nu_h^{n,m} \in Z_h$ the approximate viscosity $\Pi_h[\nu^n(\theta_h^m)]$. Similarly, $\kappa_h^{n,m}$, $\sigma_h^{n,m}$, and $\beta_h^{n,m}$ are defined, where Z_h is a finite dimensional subspace of Q and Π_h an interpolation to Z_h.

Hereafter, the boundary data u_D, θ_D, and ϕ_D are assumed to be independent of time. We introduce an approximate problem discretized by the backward Euler method in time and by the finite element method in space: Setting $\theta_h^0 \in \Psi_h(\theta_D)$ as an approximation to θ^0, we find $\{(u_h^n, p_h^n, \theta_h^n, \phi_h^n) \in V_h(u_D)\times$

$Q_h \times \Psi_h(\theta_D) \times \Xi_h(\phi_D);\ n = 1, \ldots, N_T\}$ such that for $n = 1, \ldots, N_T$

$$\begin{cases} a_0(\nu_h^{n,n-1}; u_h^n, v_h) + b(v_h, p_h^n) \\ \qquad\qquad -(\beta_h^{n,n-1}\,\theta_h^{n-1},\, v_h) = 0 & \text{for all } v_h \in V_h, \quad (3.1a) \\ b(u_h^n, q_h) = 0 & \text{for all } q_h \in Q_h, \quad (3.1b) \\ (\overline{D}_\tau \theta_h^n,\, \psi_h) + c_0(\kappa_h^{n,n-1}; \theta_h^n,\, \psi_h) \\ \qquad + c_1(u_h^{n-1}, \theta_h^n,\, \psi_h) = \dfrac{1}{2}(\sigma_h^{n,n-1} |\overline{\nabla \phi}_h^n|^2,\, \psi_h) & \text{for all } \psi_h \in \Psi_h, \quad (3.1c) \\ \widetilde{c}_0(\widetilde{\sigma}_h^{n,n-1}; \phi_h^n,\, \xi_h) = 0 & \text{for all } \xi_h \in \Xi_h. \quad (3.1d) \end{cases}$$

At nth time step, the approximate problem is split up into three parts; one is the Stokes part (3.1a) and (3.1b), another the generalized convection-diffusion part (3.1c), and the other the Poisson part (3.1d). Assuming some conditions to choose a pair of finite elements $(X_h,\ Q_h,\ \widetilde{X}_h,\ Z_h)$, we can prove the solvability of (3.1); for detail, see [4] and [6]. As a result, the solution $\{(u_h^n, p_h^n, \theta_h^n, \phi_h^n)\}$ is obtained step by step from θ_h^0.

4. Numerical results

Set $T = 0.5$. The physical coefficients ν, κ, σ, and β are defined by

$$\nu \equiv 0.01 \exp\Big(\frac{50}{10+\theta}\Big), \qquad \kappa \equiv 0.01\,\theta^2 + 0.2\,\theta + 1,$$
$$\sigma \equiv 55 \exp\Big(\frac{-50}{15+\theta}\Big), \qquad \beta \equiv (0,\ 20000).$$

These coefficients are obtained by normalizing with 1500 [K] and by rounding those of a raw glass material given in [7]. For detail of the normalization, see [5]. From this normalization, the values of unknown functions lie roughly in

$$-4 \times 10^2 \lesssim u_1 \lesssim 2 \times 10^3, \qquad -4 \times 10^2 \lesssim u_2 \lesssim 1 \times 10^3,$$
$$-3 \times 10^{-6} \lesssim p \lesssim 5 \times 10^5, \qquad -3 \lesssim \theta,\ \phi \lesssim 4.$$

Figure 2 shows the graph of ν, κ, and σ versus the temperature. Table 2 shows the common control data

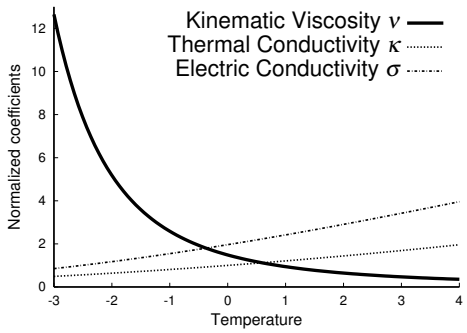

Figure 2. The temperature-dependent coefficients.

for u and θ on the boundary and at the initial time, which are also normalized with 1500 [K]. Table 3

lists three cases of the electric potential values on $\widetilde{\Gamma}_E$. In each case, the sum of the values is equal to 0. In Case A, the values are obtained by normalizing and rounding the root-mean-square values of the complex potentials given in [7]. For detail of the normalization, see [5] again. In Cases B and C, the locations of the positive potential are different from those in Case A.

Table 2
The common control data for u and θ on the boundary and at the initial time.

Place	u	Place	θ	Time	θ
Γ_W	(0, 0)	Γ_B	-3	$t = 0$	0
Γ_B	(400, 8)	Γ_S	3		

Table 3
The electric potential ϕ imposed on $\widetilde{\Gamma}_E$.

Case	$\widetilde{\Gamma}_{E_1}$	$\widetilde{\Gamma}_{E_2}$	$\widetilde{\Gamma}_{E_3}$
A	6	-3	-3
B	-3	6	-3
C	-3	-3	6

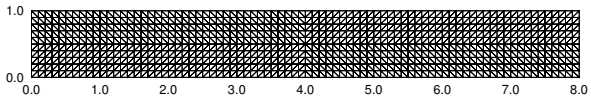

Figure 3. The cross section Ω and its triangulation.

The domain $\widetilde{\Omega}$ is divided into a union of $80 \times 10 \times 10$ cuboides, and each cuboid is divided into 6 tetrahedra, that is, the domain $\widetilde{\Omega}$ is divided into a union of $48,000$ tetrahedra. Figure 3 shows the triangulation of Ω. We denote the maximum diameter of the triangles by $h = \sqrt{2}/10 \approx 0.14$. To approximate the velocity, the pressure, the temperature, and the electric potential, the finite elements $P2/P1/P2/P2$ are used, which have the second order approximability; see [4]. The physical coefficients are approximated by $P1$ elements, which is the most efficient choice; see also [4]. The time increment τ is set to be $\tau = 4.0 \times 10^{-3}$ so that the size of τ may resolve the period of oscillation phenomena in the following Figure 5.

At each step, the Stokes part (3.1a) and (3.1b) and the generalized convection-diffusion part (3.1c) were solved by the Gauss elimination method, and the Poisson part (3.1d) was solved by the Conjugate Gradient (CG) method with the incomplete LU factorization preconditioner. The CG method was stopped when its relative residual becomes less than 10^{-8}. The computation was performed by Pentium4 3.2GHz with 2GB memories. In each case, it took about 5 hours to compute.

Figure 4 shows the streamlines, the temperature, and the electric potential at 0.16-time-intervals in Case A. At $t = 0.02$, there is a large roll cell under the batch, and the raw material is not yet fully

heated. As the time goes by, there appears a series of roll cells, which become weak in approaching the throat.

Figure 5 shows the history of a Joule heat J and an energy E defined by

$$J \equiv \frac{1}{2}\int_{\Omega} \sigma(\theta)|\overline{\nabla\phi}|^2 \, dx, \qquad E \equiv \int_{\Gamma_T} u_1 \, \theta \, ds.$$

In Figure 5(b), for the comparison, there is also the graph in the case without the Joule heat, "Without Rods". The averages of the energies in Cases A, B, and C are about 1.08 times lager than that in "Without Rods". The periodic motion of the convection phenomena causes the oscillation of J and E. The amplitudes of E when an electric current flows becomes smaller than those when a current does not; the amplitude of E in "Without Rods" is about 10–15% of the value of E itself; on the other hand, those in Cases A, B, and C are about 2–3%. The period of these oscillations is about 0.008–0.012. Figure 6 shows the electric potential on $x_3 = 0.3$ in Cases A and B. From Figure 6 the gradient of the electric potential on $x_2 = 0$ in Case B is less than that in Case A. This fact imply, as in Figure 5, the Joule heat in Case B is about half of those in Cases A and C. Figure 7 shows the streamlines and the temperature near the throat. The upper figure shows the result when the oscillation of the energy achieves a trough at $t = 0.408$. The lower figure shows the result when the oscillation of the energy achieves a peak at $t = 0.416$. The pattern of the streamlines at the peak is distinguished from that at the trough. The center of the nearest role cell to the throat is about $6.3 \leq x_1 \leq 6.7$ at the trough, and is about $7.1 \leq x_1 \leq 7.2$ at the peak. The distributions of the temperature, meanwhile, are almost same at both the peak and the trough. These facts imply that the periodic motion of the flow is related to those of J and E.

Table 4 shows the Joule heat and the energy consumptions. "Given" and "Out" mean the Joule heat G on $x_2 = 0$ and the energy O passing the throat defined by

$$G \equiv \int_0^T J \, dx, \qquad O \equiv \int_0^T \int_{\Gamma_T} u_1 \, (\theta - \theta_0) \, ds,$$

respectively. Here θ_0 is the temperature in the case without the electrodes. "Ratio" is defined by the ratio of "Out" to "Given". This table shows that both Joule heat and "Out" energy in Case C are the highest among the three cases. As mentioned in Figure 6, the Joule heat in Case B is about a half of those in the other cases. "Ratio" in Case C is 1.3–1.6 times as high as those in the other cases. As a result, Case C is the best configuration among the cases.

Table 4
The energy consumptions in each case.

Case	Given	Out	Ratio [%]
A	19.9	1.13	5.70
B	9.3	0.43	4.63
C	20.2	1.47	7.25

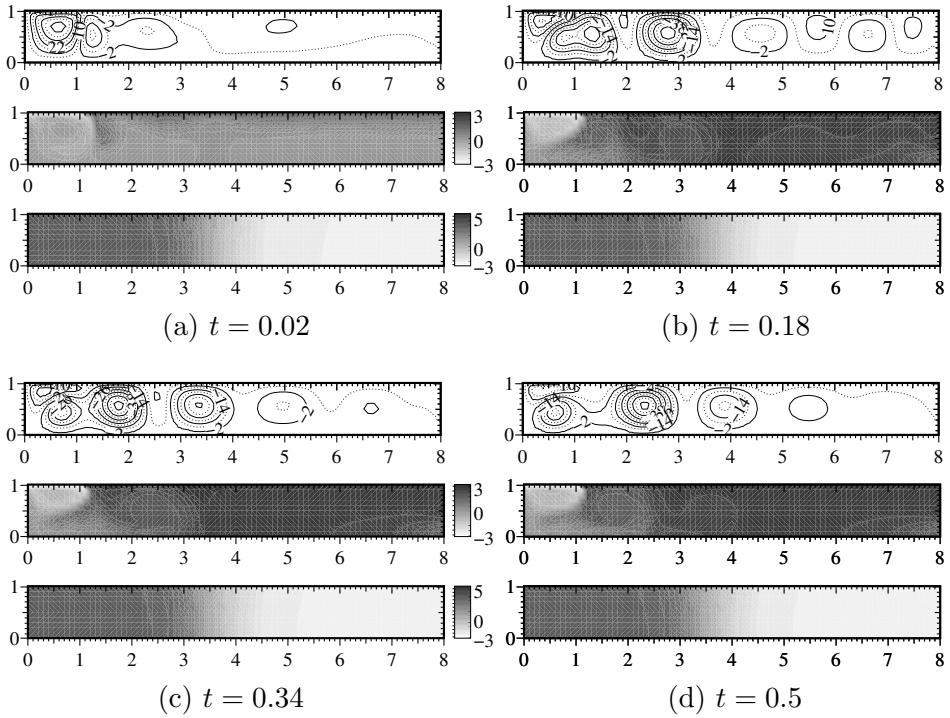

Figure 4. The streamlines (Upper), the temperature (Middle), and the electric potential (Lower) in Case A.

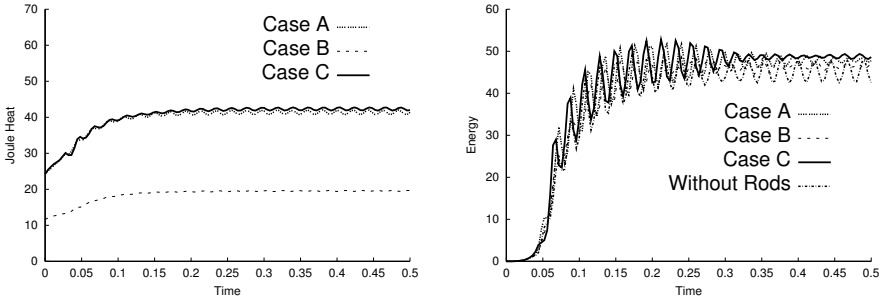

(a) The Joule heat J. (b) The energy E.

Figure 5. The Joule heat on $x_2 = 0$ and the energy at the throat.

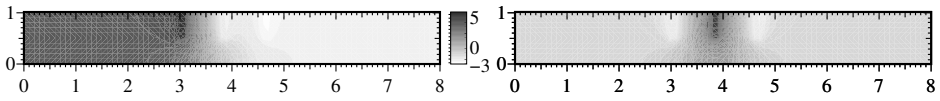

Figure 6. The electric potential in Cases A (left) and B (right) on $x_3 = 0.3$.

5. Concluding remarks

In this paper we have computed a melting glass convection in a model furnace by a finite element method derived from [3]–[6]. Some numerical results have been demonstrated to investigate differences of the energy efficiency among some electrode configurations.

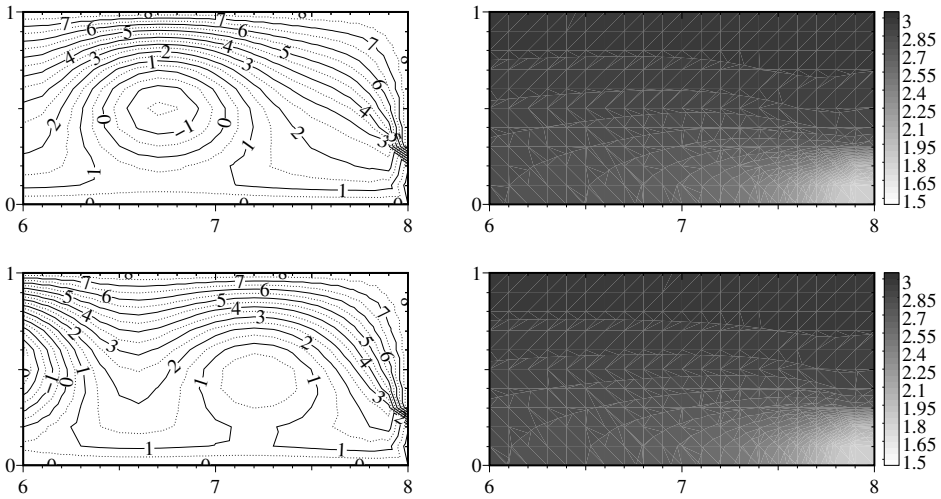

Figure 7. The streamlines (Left) and the temperature (Right) near the throat in Case A at $t = 0.408$ (Above) and 0.416 (Below).

In this paper we simplify a part of the problem and solve the heat convection equations in a cross section. We are going to solve the whole problem in the three-dimensional configuration.

Acknowledgment: The authors thank Dr. Hajime Itoh of Asahi Glass Co., Ltd. for giving us useful information on the glass furnaces. This work was supported by the Japan Society for the Promotion of Science under Grants-in-Aid for Scientific Researches (B), No.15360044 and (S), No.16104001 and by the Ministry of Education, Culture, Sports, Science and Technology of Japan under Kyushu University 21st Century COE Program, Development of Dynamic Mathematics with High Functionality.

References

[1] Choudhary, M., *Three-dimensional mathematical model for flow and heat transfer in electric glass furnaces*, Heat Transfer Eng. **6** (1985), 55–65.

[2] Curran, R. L., *Use of mathematical modeling in determining the effects of electrode configuration on convection currents in an electric glass melter*, IEEE Trans. Ind. Gen. Appl. **IGA-7** (1971), 116–129.

[3] Tabata, M., *Finite element approximation to infinite Plandtl number Boussinesq equations with temperature-dependent coefficients—thermal convection problems in a spherical shell*, to appear in Future Gener. Comput. Syst.

[4] Tabata, M. and Tagami, D., *Error estimates of finite element methods for nonstationary thermal convection problems with temperature-dependent coefficients*, Numer. Math. **100** (2005), DOI 10.1007/s00211-005-0589-2, In press.

[5] Tagami, D., *A finite element analysis of thermal convection problems with the Joule heat*, Ph.D. thesis, Kyushu University, 2003.

[6] Tagami, D. and Itoh, H., *A finite element analysis of thermal convection problems with the Joule heat*, Japan J. Indust. Appl. Math. **20** (2003), 193–210.

[7] Ungan, A. and Viskanta, R., *Three-dimensional numerical simulation of circulation and heat transfer in an electrically boosted glass melting tank*, IEEE Trans. Ind. Appl. **IA-22** (1986), 922–933.

[8] Viskanta, R. and Anderson, E. F., *Heat transfer in semitransparent solids*, Adv. Heat Transfer **11** (1975), 317–441.

List of MHF Preprint Series, Kyushu University

21st Century COE Program
Development of Dynamic Mathematics with High Functionality

MHF2003-1 Mitsuhiro T. NAKAO, Kouji HASHIMOTO & Yoshitaka WATANABE
A numerical method to verify the invertibility of linear elliptic operators with applications to nonlinear problems

MHF2003-2 Masahisa TABATA & Daisuke TAGAMI
Error estimates of finite element methods for nonstationary thermal convection problems with temperature-dependent coefficients

MHF2003-3 Tomohiro ANDO, Sadanori KONISHI & Seiya IMOTO
Adaptive learning machines for nonlinear classification and Bayesian information criteria

MHF2003-4 Kazuhiro YOKOYAMA
On systems of algebraic equations with parametric exponents

MHF2003-5 Masao ISHIKAWA & Masato WAKAYAMA
Applications of Minor Summation Formulas III, Plücker relations, Lattice paths and Pfaffian identities

MHF2003-6 Atsushi SUZUKI & Masahisa TABATA
Finite element matrices in congruent subdomains and their effective use for large-scale computations

MHF2003-7 Setsuo TANIGUCHI
Stochastic oscillatory integrals - asymptotic and exact expressions for quadratic phase functions -

MHF2003-8 Shoki MIYAMOTO & Atsushi YOSHIKAWA
Computable sequences in the Sobolev spaces

MHF2003-9 Toru FUJII & Takashi YANAGAWA
Wavelet based estimate for non-linear and non-stationary auto-regressive model

MHF2003-10 Atsushi YOSHIKAWA
Maple and wave-front tracking — an experiment

MHF2003-11 Masanobu KANEKO
On the local factor of the zeta function of quadratic orders

MHF2003-12 Hidefumi KAWASAKI
Conjugate-set game for a nonlinear programming problem

MHF2004-1 Koji YONEMOTO & Takashi YANAGAWA
Estimating the Lyapunov exponent from chaotic time series with dynamic noise

MHF2004-2 Rui YAMAGUCHI, Eiko TSUCHIYA & Tomoyuki HIGUCHI
State space modeling approach to decompose daily sales of a restaurant into time-dependent multi-factors

MHF2004-3 Kenji KAJIWARA, Tetsu MASUDA, Masatoshi NOUMI, Yasuhiro OHTA & Yasuhiko YAMADA
Cubic pencils and Painlevé Hamiltonians

MHF2004-4 Atsushi KAWAGUCHI, Koji YONEMOTO & Takashi YANAGAWA
Estimating the correlation dimension from a chaotic system with dynamic noise

MHF2004-5 Atsushi KAWAGUCHI, Kentarou KITAMURA, Koji YONEMOTO, Takashi YANAGAWA & Kiyofumi YUMOTO
Detection of auroral breakups using the correlation dimension

MHF2004-6 Ryo IKOTA, Masayasu MIMURA & Tatsuyuki NAKAKI
A methodology for numerical simulations to a singular limit

MHF2004-7 Ryo IKOTA & Eiji YANAGIDA
Stability of stationary interfaces of binary-tree type

MHF2004-8 Yuko ARAKI, Sadanori KONISHI & Seiya IMOTO
Functional discriminant analysis for gene expression data via radial basis expansion

MHF2004-9 Kenji KAJIWARA, Tetsu MASUDA, Masatoshi NOUMI, Yasuhiro OHTA & Yasuhiko YAMADA
Hypergeometric solutions to the q - Painlevé equations

MHF2004-10 Raimundas VIDŪNAS
Expressions for values of the gamma function

MHF2004-11 Raimundas VIDŪNAS
Transformations of Gauss hypergeometric functions

MHF2004-12 Koji NAKAGAWA & Masakazu SUZUKI
Mathematical knowledge browser

MHF2004-13 Ken-ichi MARUNO, Wen-Xiu MA & Masayuki OIKAWA
Generalized Casorati determinant and Positon-Negaton-Type solutions of the Toda lattice equation

MHF2004-14 Nalini JOSHI, Kenji KAJIWARA & Marta MAZZOCCO
Generating function associated with the determinant formula for the solutions of the Painlevé II equation

MHF2004-15 Kouji HASHIMOTO, Ryohei ABE, Mitsuhiro T. NAKAO & Yoshitaka WATANABE
Numerical verification methods of solutions for nonlinear singularly perturbed problem

MHF2004-16 Ken-ichi MARUNO & Gino BIONDINI
Resonance and web structure in discrete soliton systems: the two-dimensional Toda lattice and its fully discrete and ultra-discrete versions

MHF2004-17 Ryuei NISHII & Shinto EGUCHI
Supervised image classification in Markov random field models with Jeffreys divergence

MHF2004-18 Kouji HASHIMOTO, Kenta KOBAYASHI & Mitsuhiro T. NAKAO
Numerical verification methods of solutions for the free boundary problem

MHF2004-19 Hiroki MASUDA
Ergodicity and exponential β-mixing bounds for a strong solution of Lévy-driven stochastic differential equations

MHF2004-20 Setsuo TANIGUCHI
The Brownian sheet and the reflectionless potentials

MHF2004-21 Ryuei NISHII & Shinto EGUCHI
Supervised image classification based on AdaBoost with contextual weak classifiers

MHF2004-22 Hideki KOSAKI
On intersections of domains of unbounded positive operators

MHF2004-23 Masahisa TABATA & Shoichi FUJIMA
Robustness of a characteristic finite element scheme of second order in time increment

MHF2004-24 Ken-ichi MARUNO, Adrian ANKIEWICZ & Nail AKHMEDIEV
Dissipative solitons of the discrete complex cubic-quintic Ginzburg-Landau equation

MHF2004-25 Raimundas VIDŪNAS
Degenerate Gauss hypergeometric functions

MHF2004-26 Ryo IKOTA
The boundedness of propagation speeds of disturbances for reaction-diffusion systems

MHF2004-27 Ryusuke KON
Convex dominates concave: an exclusion principle in discrete-time Kolmogorov systems

MHF2004-28 Ryusuke KON
Multiple attractors in host-parasitoid interactions: coexistence and extinction

MHF2004-29 Kentaro IHARA, Masanobu KANEKO & Don ZAGIER
Derivation and double shuffle relations for multiple zeta values

MHF2004-30 Shuichi INOKUCHI & Yoshihiro MIZOGUCHI
Generalized partitioned quantum cellular automata and quantization of classical CA

MHF2005-1 Hideki KOSAKI
Matrix trace inequalities related to uncertainty principle

MHF2005-2 Masahisa TABATA
Discrepancy between theory and real computation on the stability of some finite element schemes

MHF2005-3 Yuko ARAKI & Sadanori KONISHI
Functional regression modeling via regularized basis expansions and model selection

MHF2005-4 Yuko ARAKI & Sadanori KONISHI
Functional discriminant analysis via regularized basis expansions

MHF2005-5 Kenji KAJIWARA, Tetsu MASUDA, Masatoshi NOUMI, Yasuhiro OHTA & Yasuhiko YAMADA
Point configurations, Cremona transformations and the elliptic difference Painlevé equations

MHF2005-6 Kenji KAJIWARA, Tetsu MASUDA, Masatoshi NOUMI, Yasuhiro OHTA & Yasuhiko YAMADA
Construction of hypergeometric solutions to the q - Painlevé equations

MHF2005-7 Hiroki MASUDA
Simple estimators for non-linear Markovian trend from sampled data:
I. ergodic cases

MHF2005-8 Hiroki MASUDA & Nakahiro YOSHIDA
Edgeworth expansion for a class of Ornstein-Uhlenbeck-based models

MHF2005-9 Masayuki UCHIDA
Approximate martingale estimating functions under small perturbations of dynamical systems

MHF2005-10 Ryo MATSUZAKI & Masayuki UCHIDA
One-step estimators for diffusion processes with small dispersion parameters from discrete observations

MHF2005-11 Junichi MATSUKUBO, Ryo MATSUZAKI & Masayuki UCHIDA
Estimation for a discretely observed small diffusion process with a linear drift

MHF2005-12 Masayuki UCHIDA & Nakahiro YOSHIDA
AIC for ergodic diffusion processes from discrete observations

MHF2005-13 Hiromichi GOTO & Kenji KAJIWARA
Generating function related to the Okamoto polynomials for the Painlevé IV equation

MHF2005-14 Masato KIMURA & Shin-ichi NAGATA
Precise asymptotic behaviour of the first eigenvalue of Sturm-Liouville problems with large drift

MHF2005-15 Daisuke TAGAMI & Masahisa TABATA
Numerical computations of a melting glass convection in the furnace